Synthetic Routes for the Preparation of Ordered Vanadium Oxide Inverted Opal Electrodes for Li-ion Batteries

E. Armstrong[1], W. Khunsin[2], C. M. Sotomayor Torres[2], M. Osiak[1] and C. O'Dwyer[1,3]

Department of Chemistry, University College Cork, Cork, Ireland
[2]Catalan Institute of Nanoscience and Nanotechnology ICN2, Campus UAB, Edifici ICN2, 08193 Bellaterra, Spain
[3]Micro and Nanoelectronics Centre, Tyndall National Institute, Lee Maltings, Cork, Ireland

Synthetic routes for the formation of opal assemblies as templates for the inverted opal vanadium oxide electrodes are presented. A method for the formation of monolayer opal templates on gold substrates is discussed and the formation of multilayer opal templates on conductive substrates by electrophoretic deposition is also described, with order defined by angle resolved light scattering measurements. Inverted opals are formed from a diluted solution of IPA and vanadium alkoxide precursor, infiltrated into the templates by several methods. The effect of different heat treatments and method of polymer template removal on the resulting inverse opal morphology and structure is investigated.

Introduction

The demand for light weight electric power sources capable of delivering both high energy and high power density is higher than ever, due in most part to the rapid growth in portable devices and the increasing need for hybrid vehicles. Lithium ion battery cells, which offer specific energies higher than other electrochemical power sources, have become the leading battery type for many of these applications (1). There has been extensive research into what materials, designs and techniques will deliver the sustainable energy storage needed for next generation battery devices. One design presently showing great promise as a flexible and interconnected architecture for lithium-ion battery cathodes is bi-continuous three-dimensionally ordered macroporous (3DOM) electrodes (2). These have been shown to offer improvements in rate performance and conductivity by increasing the surface area available for electrolyte contact and lowering the need for conductive additives alleviating some of the issues presently impeding research developments such as poor ion diffusion, electrical disconnection, and battery dead weight (3). A number of approaches to the use and formation of these three dimensional porous architectures have been taken, such as, interdigitated electrodes (4), sponge geometries and that of inverted opal structures formed through the use of opal templates (5).

The control over pore size, geometry and the adaptability to a variety of materials make inverted opal structures of particular interest. Templating is usually done using colloidal crystals composed of mono-dispersed spheres and assembled using a variety of well-controlled methods (6), such as spin-coating (7), drop-casting (8), vertical deposition (9), electrophoretic deposition (10), dip-coating and Langmuir Blodgett (11, 12) or layer-by-layer assembly (13). Infiltration of the active material into the empty volume between the spheres and removal of the template produces the inverted opal design. The degree of choice available in terms of the assembly of the colloidal crystal template, infiltration and processing, template removal, and other necessary modifications to enhance the functionality

of the materials, make these ideal structures for application as lithium ion battery electrodes, both as cathodes and anodes (14).

Another important consideration is the choice of material for the electrode. Looking at the cathode material in particular, one of the more promising, is that of vanadium oxide, the intercalation properties of which have been investigated significantly over the last 30 years (15). Vanadium pentoxide has a layered structure and weak vanadium-oxygen bonds between the layers which allows for easy accommodation for the lithium ions. This increased capacity combined with its low cost, abundance, ease of synthesis and more specifically its high energy efficiency make it an attractive cathode material for use in lithium ion battery cathodes. However, the use of vanadium oxide has been largely limited by poor electron conductivity and the significant structural changes caused by the lithium insertion. Volumetric expansion and the subsequent loss of mechanical integrity and decrease in capacity is a major difficulty one that the inverted opal structure has the potential to alleviate (16). There are limited means of investigation towards optimizing electrochemical performance at ultrafast rates and the photonic abilities of these inverted opal structures provide a means of optically probing structural and phase changes by monitoring variations in the scattering ability of the material on lithium insertion.

In this paper, we present an approach to the formation of a series of opal templates both 2-dimensional (2D) structures on gold substrates formed by dip-coating and 3-dimensional (3D) templates on conductive substrates such as ITO coated glass and gold substrates by electrophoretic deposition. Vanadium oxide IO battery cathodes with different morphologies are also created by infiltration with the alkoxide precursor diluted with isopropanol and subsequent removal of the spheres. The influence of the method of infiltration and removal of the spheres, and any heat treatment for material crystallization is discussed and the potential application of these structures in the development of optical probing of structural changes in Li-ion battery materials.

Experimental

Polystyrene sphere template preparation

Poly(methylmethacrylate) (PMMA) spheres of 700 nm in diameter (D) were prepared by the emulsion polymerization procedure described elsewhere (17), these were then centrifuged and dried at 50°C and redistributed in distilled water to form a solution of 5 wt% concentration. The surfactant sodium dodecyl sulphate (SDS) was then added to this solution at a concentration of 8 mg ml^{-1} above the theoretical critical micelle concentration (CMC) for SDS of 2.3 mg ml^{-1} (8.0×10^{-3} mol dm^{-3}). A silicon wafer was cleaned in argon plasma and coated with 10 nm titanium adhesion layer and 100-150 nm gold by ion beam sputtering using an ATC Orion-5-UHV sputtering system. A piece approximately 1 cm × 1 cm was then cleaned by sonication in acetone, ethanol, and rinsed with deionized water. The sample was then settled vertically in the solution of spheres and withdrawn at a rate of 1 mm/min.

Electrophoretic deposition was used to prepare multi-layered templates. Briefly, 0.8 ml of sulphated spheres i.e. with a net negative charge, suspended in water were mixed with 3.2 ml of ethanol (this was adjusted between deposits to ensure complete coverage of sample area). This formed ~ 4 ml of solution with 1.25% spheres concentration. To adjust the pH of the mixture to ~10, ammonium hydroxide was added to the solution. The electrodes were of ITO glass and gold coated silicon and were prepared by washing in acetone, ethanol, and deionized water by sonication. The electrodes were kept at a constant distance of 5 mm from a counter electrode of aluminium and were kept completely in parallel. The electrophoretic

deposition was carried out at 2.5 V applied for a variety of times and then compared. The templates were dried in air.

Inverted opals were prepared by direct infiltration of the opal templates by a number of methods and subsequent removal of the template material. Briefly, isopropanol was mixed with deionized water in the ratio of 100:0.1 and then vanadium triisopropoxide oxide ($OV(OCH(CH_3)_2)_3$) was added to this IPA and water solution. This 100:1:0.1 precursor was then directly applied to the opal template. Following the precursor application, the templates were treated either by calcination and/or crystallization in a furnace, an oven, or by UV-ozone treatment.

Characterization of the opal templates was performed using scanning electron microscopy (SEM), performed on a Hitachi S-4800 field emission SEM, and this was used to visualize the in-plane (top layer) ordering of the samples. The depth of ordering was probed by angle-resolved spectroscopy in a monochromator-mount configuration on a rotating stage with fixed incident angles of 60° and 45°. The sample was illuminated with white light from a Halogen bulb collimated to a beam diameter of ~1 mm. Spectra of the planar diffracted light were collected at an interval of 5° and an angular resolution of 2° using a CCS200 Compact CCD spectrometer in the wavelength range 200 – 1000 nm.

Results and discussion

Figure 1a shows a schematic outlining the electrophoretic deposition of the PS spheres. This produced well-ordered templates confirmed by the clearly visible (111) face formed parallel to the substrate, the (111) plane forms preferentially to other planes due to lowest energy (maximum packing) for the spheres in this arrangement. Increasing the time of deposition increases the thickness with an eventual saturation point reached whereby the deposited spheres begin to screen the charge from the substrate electrode and so begin hindering the attractive forces induced on the negatively charged spheres. Local lattice distortions or vacancy defects in the order can be conveniently traced back to particle size distribution and shrinkage of the spheres during the drying process, a common cause of cracks usually observed in 3D PhCs by colloidal self-assembly with a large volume fraction of water.

Two-dimensional (2D) monolayer opal templates were formed by the addition of the surfactant sodium dodecyl sulphate (SDS) during dip-coating at a rate of 1 mm/min. The dissociation of this amphilic anion in water produces charged monomers, and at a sufficiently high concentration, greater than the critical micelle concentration (CMC), these monomers form micelles, their hydrophobic tails group together forming a hydrophobic core and their hydrophilic heads orientate towards the polar solute. Micelles are known to enhance and alter certain characteristics of a solution e.g. the solubility of hydrophobic materials, viscosity and polarity.(18) In our experiment, SDS was used at a concentration of 8 mg ml^{-1} (> CMC), above the theoretical CMC for SDS of 2.3 mg ml^{-1} (8.0×10^{-3} mol dm^{-3}) and at room temperature.(30) The formation of micelles in the solution caused an improvement in the order observed in the resulting template, due to a combination between the repulsive electrostatic forces induced beyond the Debye screening length in the electrical double layer and depletion force kinetics.

The deposition was performed with a fast withdrawal rate of 1 mm/min, and SEM confirmed the resulting hexagonally packed monolayer of spheres. Figure 1e shows the angle-resolved diffraction measurement obtained at angular increments of 5° for light incident at 60°. Confirmation of the structure of the 2D monolayer opal template formed by

this method is provided by analysis of this angle-resolved diffraction. It conforms very well with the planar grating equation, $\lambda = d[\sin(\alpha)+\sin(\beta+x)]$, where α is the angle of incidence, β is the angle of diffraction, d is the effective grating groove, which in this case corresponds to $\sqrt{3}/2$ D, the half period of the trigonal lattice for the wave vector of incident light propagating along the ΓK direction in the Brillouin zone of a 2D hexagonal lattice. The 2D opal template showed no three-dimensional order, evident by the lack of a photonic band gap within the expected range. In addition to lattice distortion, lattice misalignments in the monolayer 2D PhC are found to be caused mainly by the line dislocations stemming from anomalies in the close-packed 2D assembly.

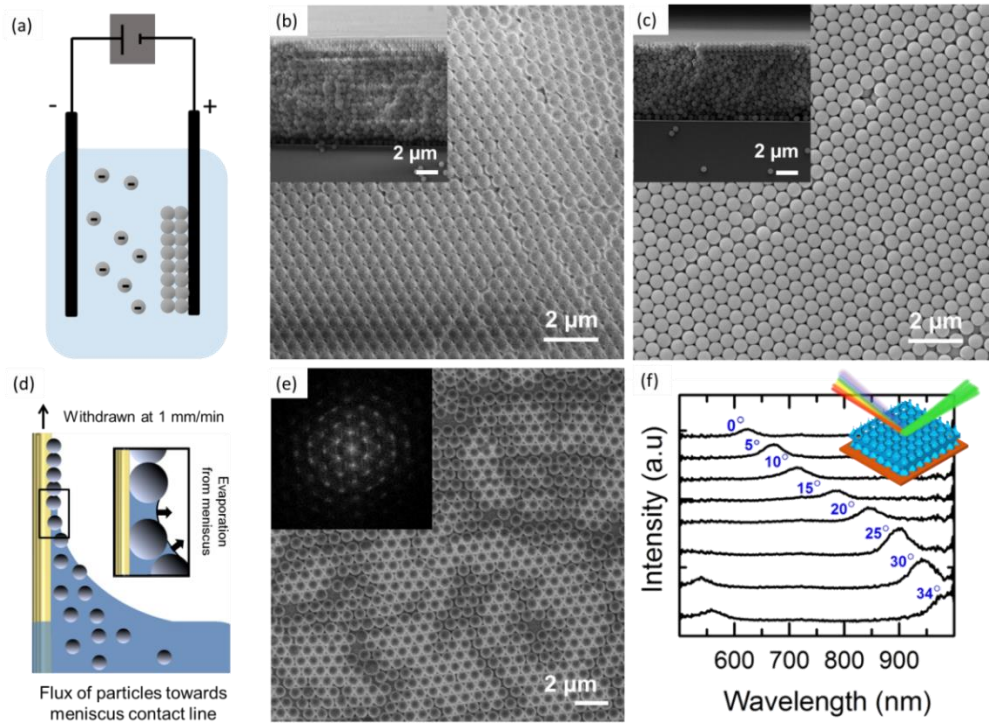

Figure 1. (a) Schematic diagram depicting EPD deposition (b) SEM image of 500 nm polystyrene spheres forming an opal template after EPD deposition of 10 min on ITO glass substrate (c) SEM image of polystyrene spheres forming opal template after EPD deposition of 10 min on gold coated silicon substrate (d) Schematic diagram depicting dip-coating of the PMMA spheres (e) SEM image of a monolayer of 700 nm PMMA spheres formed on gold coated silicon by dip-coating, the inset shows the FFT of this image indicating a resemblance to ordered crystalline diffraction pattern (f) 2D diffraction from the opal monolayer in (e), the schematic describes the method: white light is directed onto the sample and certain wavelengths of light, dependent on the order and porosity of the material are reflected.

After the template preparation, infiltration of the precursor was performed by a variety of methods with the objective of obtaining a vanadium oxide inverted opal that maintains some degree of the order and structural integrity of the template used to create it. Predefining order is a requirement for probing the photonic band gap or scattering in inverted opal electrodes that change during lithium insertion and removal. The first method involved the pre-made template. The dried spheres were mixed with the precursor solution and drop casted as a whole on to a silicon substrate. Drop-casting of an aqueous solution of PS spheres will usually orientate into ordered domains but is not a favoured technique due to limited control over the coverage and order. This method helps identify if any ordering takes place

during the drying of the precursor, therefore forming template and material architecture simultaneously. This sample was allowed to dry in air and template removal was performed in a furnace for 5 h at 450 °C. The high temperature of the template removal accelerates and finalizes the process of hydrolysis of the vanadium oxide precursor and crystallizes the initially amorphous vanadium oxide inverted opal walls. This method resulted in an inverted opal morphology, shown in Fig. 2a, with limited ordering. FFT analysis (inset) confirms a dominant 'polycrystalline' order within the (111) plane of an fcc lattice of voids after template removal from the composite template/precursor mixture during heating. The spheres were removed but it is plausible that rapid formation and crystallization of the vanadium oxide walls during its condensation from the decomposing alkoxide, together with the initial level of disorder in the opal template from drop-casting produced a widely varied morphology across the substrate.

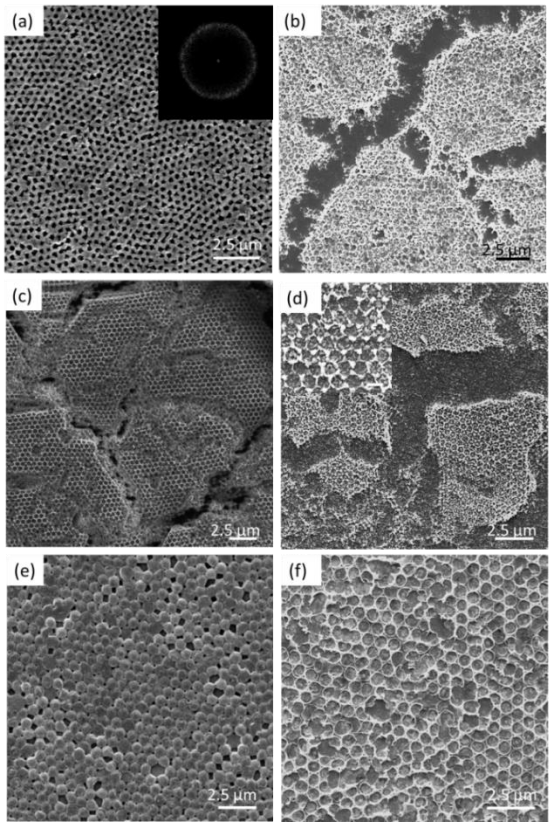

Figure 2. SEM images of inverted opals prepared by (a) Drop-cast pre-mixed PS sphere and precursor solution on silicon substrate and calcined at 450°C for 5 h, the FFT for this image is shown in the inset, a completely amorphous pattern is shown (b) Drop-cast precursor solution under sonication on to multilayer PS template and calcined at 450°C for 5 h (c) Multilayer PS template dip-coated (200 mm/min × 4) with the 100:1:0.1(IPA: $OV(OCH(CH_3)_2)_3$ precursor: deionized water solution at 200 mm/min and UV-ozone applied for 3 h (d) Sample from (c) after calcination at 450 °C for 3h to remove the spheres fully and crystallize the vanadium oxide (e) Dip coated (150 mm/min × 6) monolayer template after UV Ozone for 6 h, spheres still present (f) Dip coated (150 mm/min × 6) monolayer template after UV Ozone for 12 hours.

The use of a pre-fabricated opal multilayer (3D) and monolayer (2D) templates with direct drop casting of the precursor solution also yielded corresponding inverted opals structures of vanadium oxide. Firstly, this was done on a multilayer sample under sonication. The sample was then dried in air and calcined in a furnace for 5 h at 450 °C. The resulting

film, shown in Fig. 2b was thin and of varied morphology, in some areas remnants of an inverted structure appear almost maintained, but the overall morphology consists of thin widely dispersed islands of material with poorly defined walls. This separation into islands is due to the removal of solvent and liquids from the porous materials as the alkoxide converts to oxide, which typically results in shrinkage causing the characteristic cracking observed that then develops into wider material voids between domains. The lower thickness compared to the original opal template and lack of inverted opal definition is likely due to the formation of thin film over-layers on deposition that form on the surface of the opal template due to hydrolysis of the material before complete infiltration.

Figures 2c and d show a sample dip coated in precursor solution and subjected first to UV-ozone treatment for 3 h (Fig. 2c) and then briefly calcined for 3 h at 450 °C. UV-ozone for 3 h was sufficient to remove only the first layer of spheres. Subsequent calcination removed the remaining sphere template forming a vanadium oxide inverted opal structure with poorly defined walls and sparse substrate coverage. The dip-coated monolayer underwent UV-ozone treatment and this was not sufficient time to fully remove the spheres (Fig. 2e), in a thinner opal template with a lower number of layers. However, when applied for 12 h this produced an inverted structure which maintained a superior structural quality, providing a monolayer inverted opal layer, shown in Fig. 2f. Compared to other infiltration methods such as CVD or electrodeposition, these types of infiltrations offer the advantage of simplicity and low cost, which is desirable for up-scaled charge storage applications using porous materials with tunable thickness and fill factor (dependent on sphere diameter and assembly).

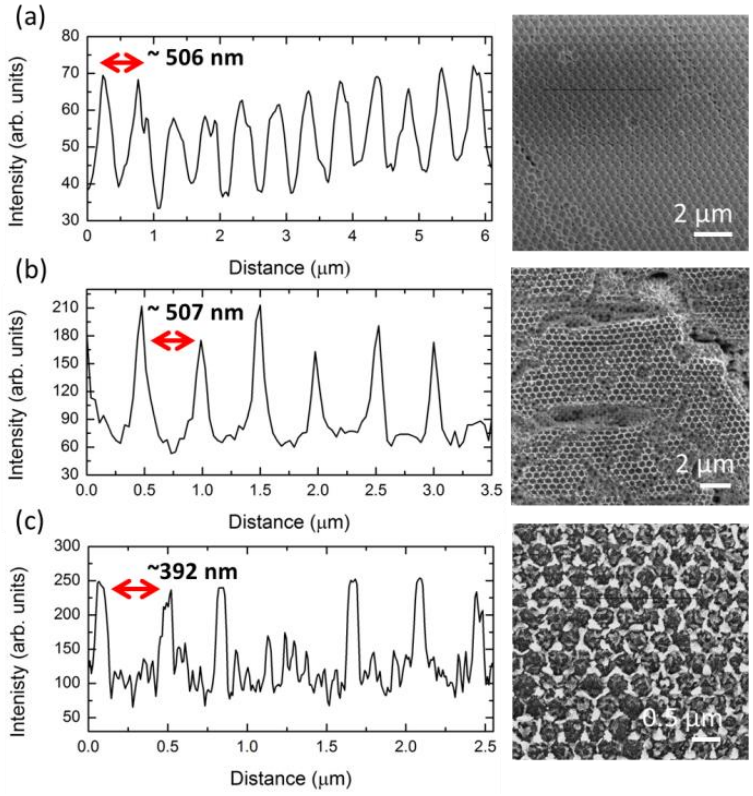

Figure 3. Line profiles for the sample shown in Fig. 2c indicating the sphere diameter for (a) an EPD template formed after 10 min, (b) the pore diameter after infiltration of this template by dip-coating and application of UV-ozone for 3 hours and (c) the subsequent calcination of this structure at 450 °C for only 3 h to remove the spheres and form crystalline V_2O_5.

Figure 3 shows a comparison of the line profiles for the template and successive UV-ozone and heat treatment outlined in Fig. 2. The corresponding structures are shown in the accompanying SEM images. This compares the template spacing i.e. sphere diameter (Fig. 3a) to that of the subsequent, inverted opals formed on only the top layer after the application of UV-ozone for 3 hours (Fig. 3b), and the remnants of inverted opals formed for this sample after further calcination in a furnace at 450 °C for 5 hours (Fig. 3c). After the UV-ozone the pore size remains unchanged; the pore size is equivalent to the sphere diameter of ~ 500 nm. This concurs with the fact that under UV-ozone the vanadium oxide is not crystallized and so experiences little morphological (and volume) change. However, after the application of high temperature and the removal of the spheres, crystallization of the vanadium oxide occurs and this causes a slight growth and disorder within the pore walls, reducing the pore size to ~ 400 nm.

Conclusions

In summary, opal templates were prepared by two methods: electrophoretic deposition and dip coating. Using these templates, inverted opal structures were prepared by a variety of methods with the aim of achieving the best structural order. It was demonstrated that the type of precursor deposition and subsequent treatment and removal of the sphere template greatly influences the morphology of the inverted opal structures composed of vanadium oxide from liquid precursors. These findings will be extended to fully describe the light scattering characteristics of the inverted opal structure as a function of the precursor deposition and treatment, and the influence lithium insertion on the structured porosity

Acknowledgments

EA and MO acknowledge the support of the Irish Research Council under awards RS/2010/2920 and RS/2010/2170. WK and CMST acknowledge support from the Spanish National I+D Plan projects TAPHOR (MAT-2012-31392) and CONSOLIDER nanoTHERM (CSD2010-00044). The authors thank Prof. J. D. Holmes for access to the Electron Microscopy Analytical Facility at Tyndall National Institute. COD acknowledges support from Science Foundation Ireland under award no. 07/SK/B1232a-STTF11, the UCC Strategic Research Fund, and from an Irish Research Council New Foundations Award.

References

1. M. S. Whittingham, *Chem. Rev.*, **104**, 4271 (2004).
2. H. Zhang, X. Yu and P. V. Braun, *Nat. Nanotechnol.*, **6**, 277 (2011).
3. A. Esmanski and G. A. Ozin, *Adv. Funct. Mater.*, **19**, 1999 (2009).
4. J. W. Long, B. Dunn, D. R. Rolison and H. S. White, *Chem. Rev.*, **104**, 4463 (2004).
5. J. H. Pikul, H. G. Zhang, J. Cho, P. V. Braun and W. P. King, *Nat. Commun.*, **4**, 1732 (2013).
6. G. von Freymann, V. Kitaev, B. V. Lotsch and G. A. Ozin, *Chem. Soc. Rev.*, **42**, 2528 (2013).
7. M. Pichumani, P. Bagheri, K. M. Poduska, W. Gonzalez-Vinas and A. Yethiraj, *Soft Matter*, **9**, 3220 (2013).
8. A. S. Dimitrov and K. Nagayama, *Langmuir*, **12**, 1303 (1996).
9. P. Jiang, J. F. Bertone, K. S. Hwang and V. L. Colvin, *Chem. Mater.*, **11**, 2132 (1999).
10. A. L. Rogach, N. A. Kotov, D. S. Koktysh, J. W. Ostrander and G. A. Ragoisha, *Chem. Mater.*, **12**, 2721 (2000).

11. B. van Duffel, R. H. A. Ras, F. C. De Schryver and R. A. Schoonheydt, *J. Mater. Chem.*, **11**, 3333 (2001).
12. M. Bardosova, P. Hodge, L. Pach, M. E. Pemble, V. Smatko, R. H. Tredgold and D. Whitehead, *Thin Solid Films*, **437**, 276 (2003).
13. J. R. Oh, J. H. Moon, S. Yoon, C. R. Park and Y. R. Do, *J. Mater. Chem.*, **21**, 14167 (2011).
14. A. Stein and R. C. Schroden, *Curr. Opin. Solid State Mater. Sci.*, **5**, 553 (2001).
15. M. S. Whittingham, *J. Electrochem. Soc.*, **123**, 315 (1976).
16. J. S. Sakamoto and B. Dunn, *J. Mater. Chem.*, **12**, 2859 (2002).
17. R. C. Schroden and N. Balakrishnan, *Inverse Opal Photonic Crystals: A Laboratory Guide*, University of Minnesota Materials Research Science and Engineering Center, University of Minnesota,Amundson Hall 491,421 Washington Ave. SE, Minneapolis, MN 55455 (2001).
18. C. C. Ruiz, *Colloids Surf., A*, **147**, 349 (1999).